

---

# **Data-Aided Fading Estimation Technique for Shadowed Mobile Satellite Fading Channels**

---

**M. H. Ng and S. W. Cheung**

Department of Electrical and Electronic Engineering

The University of Hong Kong

Hong Kong

Tel: +852 2859 2711

Fax: +852 2559 8738

Email: mhng@eee.hku.hk and swcheung@eee.hku.hk

Submitted to

**Wireless Personal Communications**

*18 May 2001*

Key words: PSA, bandwidth redundancy, fading estimation, shadowed Rician fading,

16QAM

## **ABSTRACT**

A novel data-aided fading estimation technique that employs both pilot and data symbols is proposed to significantly reduce the bandwidth redundancy of the pilot-symbol-aided (PSA) systems using receivers with low complexity and latency in the shadowed mobile satellite fading channels. The shadowed mobile satellite fading channels are modeled as the sum of a lognormally distributed direct component and a Rayleigh distributed multipath component, and the PSA system employs 16-ary quadrature-amplitude-modulation (16QAM) for transmission. Monte Carlo computer simulation has been used to assess the technique on the bit-error-rate (BER) performances of the system in the light shadowed, the average shadowed and the heavy shadowed Rician fading environments. The results have shown that the proposed technique requires a very low bandwidth redundancy to provide satisfactory BER performances, and can substantially lower the error floors of the PSA systems.

## **I. INTRODUCTION**

In digital mobile satellite communication systems, multipath fading is a major problem since it severely degrades the error rate performances and frequently causes high error floors to the systems. Pilot-symbol-aided (PSA) transmission has been proposed and studied to combat fading distortion in digital mobile communication systems [1-11]. In a PSA system, a pilot symbol from a known pseudo-random symbol sequence is multiplexed with a frame of data symbols for transmission. The receiver has a prior knowledge of the pilot symbol sequence, and so it can extract the pilot symbols from the received signal, and subsequently estimate and compensate the fading effects on the data symbols. Redundant bandwidth and power are thus required to transmit the pilot symbols. Conventional PSA fading estimation techniques make

use of only the pilot symbols but ignore the data symbols [1-9]. These estimation techniques require the use of high-order interpolating functions. When the fading rate is fast relative to the pilot symbol rate, a numerous number of pilot symbols has to be buffered and then interpolated in order to obtain the fading estimates on the data symbols, otherwise, the fading estimates become less accurate and high error floors will be incurred to the systems [3,4,7]. However, the use of high-order interpolating functions greatly increases the complexity of the receivers and, more importantly, the latency due to pilot symbol buffering which is undesirable for voice services in mobile communications. To estimate the fading distortions more accurately using low-order interpolating functions, the pilot symbols need to be sent more frequently and this increases the bandwidth redundancy of the system since more bandwidth is used to transmit the pilot symbols [4,9]. Different estimation techniques that make use of both the data symbols and the pilot symbols have been proposed [10,11]. These data-aided techniques provide better performances than the conventional techniques in the fast fading channels. One of these techniques requires the use of high-order smoothing filters to reduce the noise effects on the fading estimates obtained using the data symbols, and thus adding computational load and delay to the systems [10].

Theoretically, a fading process with a maximum Doppler spread of  $f_D$  can be sampled without distortion using the Nyquist rate of  $2f_D$  [4,5]. This means that if  $T_F$  is the pilot frame period, then  $T_F = 1/2f_D$  or  $f_D T_F = 0.5$  will be enough. With the normalized fading rates of  $f_D T = 5 \times 10^{-2}$  and  $f_D T = 2.5 \times 10^{-2}$ , where  $T$  is the channel symbol period, the frame lengths required are thus 10 and 20 symbols, respectively, leading to the bandwidth redundancies of 10% and 5%. However, in the light shadowed Rician fading environments with  $f_D T = 5 \times 10^{-2}$  and  $f_D T = 2.5 \times 10^{-2}$ , the frame lengths of 5 and 8 have been suggested [10], leading to the bandwidth

redundancies of 20% and 12.5%, respectively. Here the respective values of  $f_D T_F$  are 0.25 and 0.125, which are both smaller than the theoretical value of 0.5.

In this paper, a novel data-aided technique that employs both pilot and data symbols for fading estimation is proposed to significantly reduce the bandwidth redundancy of a PSA quadrature-amplitude-modulation (16QAM) system that uses low-order interpolating functions to obtain the fading estimates in the shadowed mobile satellite fading environments. Monte Carlo computer simulation has been used to assess the technique on the bit-error-rate (BER) performances of the system in the light shadowed, the average shadowed and the heavy shadowed Rician fading channels. The results have shown that in the shadowed Rician fading environments with  $f_D T = 5 \times 10^{-2}$  and  $f_D T = 2.5 \times 10^{-2}$ , the proposed technique requires a frame length of 50 to provide satisfactory BER performances, leading to a bandwidth redundancy of only 2%. It has also been shown that the technique can substantially lower the error floors of the PSA systems.

## II. SYSTEM MODEL

The block diagram of the land mobile satellite communication system used in this study is shown in Fig. 1. In the transmitter, a pilot symbol from a known pseudo-random symbol sequence  $\{p_{k,0}\}$  is multiplexed with every  $L-1$  data symbols to form a frame of length  $L$  as shown in Fig. 2. The data symbols  $\{d_{k,i}\}$  are possible vectors in the 16QAM signal constellation. A pseudo-random sequence of pilot symbols is used to avoid transmitting tones [1]. To minimize the fading estimation error due to additive white Gaussian noise (AWGN), the pilot symbols are chosen as the signal vectors with the highest energy levels in the signal constellation [3]. At time  $t = nT$  seconds, a data or pilot symbol is used to form an impulse  $q_n \delta(t - nT)$ , which is fed

to the premodulation filter with a square-root-raised-cosine frequency response to produce

$$s(t) = \sum_n q_n a(t - nT) \quad (1)$$

at the output, where  $a(t)$  is the impulse response of the premodulation filter.

The transmission path in Fig. 1 is a land mobile satellite fading channel that introduces shadowed Rician fading distortion to the transmitted signal. The model to generate the fading channels is shown in Fig. 3 [12], where the generated Gaussian random variables are filtered as a time series by three identical third-order Butterworth filters with the bandwidth given by  $f_D$ . The fading signal consists of a lognormally distributed line-of-sight (LOS) component and a complex Gaussian multipath component, i.e. [12]

$$y(t) = \exp[u(t)] + b'(t) + jb''(t) \quad (2)$$

where  $j = \sqrt{-1}$ ,  $u(t)$  is a Gaussian process with a mean  $\mu_0$  and variance  $d_0$ , and  $b'(t)$  and  $b''(t)$  are the zero mean Gaussian multipath components with variance  $b_0$ . The values of  $b_0$ ,  $\mu_0$  and  $d_0$  in Fig. 3 are provided in Table 1 [12]. Stationary AWGN with one-sided power spectral density of  $N_0$  is added at the input of the receiver.

At the receiver, the complex baseband signal is filtered by a postdemodulation filter, which has the same impulse response as the premodulation filter at the transmitter, to give the received signal

$$r(t) = \sum_n q_n a(t - nT) y(t) \otimes a(t) + w(t) \quad (3)$$

where  $\otimes$  denotes the convolution process,  $y(t)$  represents the fading signal, and  $w(t)$  is filtered AWGN. The baseband signal  $r(t)$  is then sampled in synchronism at the time instants  $\{nT\}$ . Assume that the fading rate is slow so that the intersymbol

interference (ISI) caused by the fading process can be neglected. Further assume that  $a(t) \otimes a(t) = 1$  at time  $t = 0$ , so the signal sample at time  $t = nT$  can be written as

$$r_n = q_n y_n + w_n \quad (4)$$

where  $q_n$  is either a pilot or data symbol, and  $y_n$  and  $w_n$  are, respectively, the fading and noise effects on  $q_n$ .

Since the receiver has a prior knowledge of the transmitted pilot symbols, the fading effects on the pilot symbols can be computed and subsequently used as the estimates of the fading effects on the data symbols. A novel fading estimation technique that can significantly reduce the bandwidth redundancy of the PSA systems is described in the following section.

### III. FADING ESTIMATION

#### *Mathematical Analysis*

Assume that frame synchronization has been achieved. The received signal at the  $i$ -th position of the  $k$ -th received frame can be written as

$$r_{k,i} = q_{k,i} y_{k,i} + w_{k,i} \quad (5)$$

where  $q_{k,i}$  is either the transmitted pilot or data symbol, and  $y_{k,i}$  and  $w_{k,i}$  are the fading effect and noise sample on the  $i$ -th symbol of the  $k$ -th frame, respectively.

The fading effects,  $y_{k,0}$  and  $y_{k+1,0}$ , on the pilot symbols,  $p_{k,0}$  and  $p_{k+1,0}$ , of the  $k$ -th and  $(k+1)$ -th frames, respectively, are estimated as

$$\hat{y}_{k,0} = \frac{r_{k,0}}{p_{k,0}} = y_{k,0} + \frac{w_{k,0}}{p_{k,0}} \quad (6a)$$

and 
$$\hat{y}_{k+1,0} = \frac{r_{k+1,0}}{p_{k+1,0}} = y_{k+1,0} + \frac{w_{k+1,0}}{p_{k+1,0}} \quad (6b)$$

By using linear interpolation [1,4],  $\hat{y}_{k,0}$  and  $\hat{y}_{k+1,0}$  can be used to estimate the fading effects on either the 1<sup>st</sup> data symbol  $d_{k,1}$  or the last data symbol  $d_{k,L-1}$  of the  $k$ -th frame. If  $d_{k,1}$  is selected, then the fading effect  $y_{k,1}$  is estimated using Eqns. (6a) and (6b) as

$$\hat{y}_{k,1} = \frac{(L-1)(y_{k,0} + w_{k,0} / p_{k,0}) + (y_{k+1,0} + w_{k+1,0} / p_{k+1,0})}{L} \quad (7)$$

which is used to compensate for the fading effect on  $r_{k,1}$  to give an estimate of  $d_{k,1}$  as

$$\hat{r}_{k,1} = \frac{r_{k,1}}{\hat{y}_{k,1}} = \frac{L(y_{k,1}d_{k,1} + w_{k,1})}{(L-1)(y_{k,0} + w_{k,0} / p_{k,0}) + (y_{k+1,0} + w_{k+1,0} / p_{k+1,0})} \quad (8)$$

The square-symbol-estimation-error (SSEE) can be expressed as

$$\begin{aligned} |e_{k,1}|^2 &= |\hat{r}_{k,1} - d_{k,1}|^2 \\ &= \left| \frac{L(y_{k,1}d_{k,1} + w_{k,1})}{(L-1)(y_{k,0} + w_{k,0} / p_{k,0}) + (y_{k+1,0} + w_{k+1,0} / p_{k+1,0})} - d_{k,1} \right|^2 \end{aligned} \quad (9)$$

At high signal-to-noise ratios (SNRs), the noise terms  $w_{k,i}$  can be neglected and Eqn. (9) is simplified to

$$\begin{aligned} |e_{k,1}|^2 &= \left| \frac{Ly_{k,1}d_{k,1} - [(L-1)y_{k,0} + y_{k+1,0}]d_{k,1}}{(L-1)y_{k,0} + y_{k+1,0}} \right|^2 \\ &= \left| \frac{d_{k,1}L(y_{k,1} - \hat{y}_{k,1})}{(L-1)y_{k,0} + y_{k+1,0}} \right|^2 \\ &= \left| \frac{d_{k,1}L \times \Delta y_{k,1}}{(L-1)y_{k,0} + y_{k+1,0}} \right|^2 \end{aligned} \quad (10a)$$

where the term  $\Delta y_{k,1}$  represents the fading estimation error. However, if the last data symbol  $d_{k,L-1}$  of the same frame is selected for fading estimation instead of  $d_{k,1}$ , then the SSEE in Eqn. (10a) becomes

$$|e_{k,L-1}|^2 = \left| \frac{d_{k,L-1} L \times \Delta y_{k,L-1}}{y_{k,0} + (L-1)y_{k+1,0}} \right|^2 \quad (10b)$$

Thus Eqns. (10a) and (10b) give the SSEE for  $d_{k,1}$  and  $d_{k,L-1}$ , respectively. Of course, the smaller is the error, the better is the estimation. Which one of the fading effects,  $y_{k,1}$  or  $y_{k,L-1}$ , should be selected for estimation depends on which of the two equations, Eqn. (10a) or (10b), gives a smaller value. Based on these findings, a novel estimation technique is proposed here to obtain a smaller square estimation error by selecting the equation, Eqn. (10a) or (10b), with the larger fading effect,  $y_{k,1}$  or  $y_{k,L-1}$ .

### *Proposed Technique*

The technique proposed in this paper selects the fading effect,  $y_{k,1}$  or  $y_{k,L-1}$ , that gives a smaller SSEE. It can be seen that the denominators of both Eqns. (10a) and (10b) consist of the fading effects  $y_{k,0}$  and  $y_{k+1,0}$ , with one of them multiplied by a factor of  $(L-1)$ . Clearly, the equation with the larger fading effect multiplied by  $(L-1)$  should have a larger denominator. Selecting the equation with a larger denominator, however, cannot guarantee a smaller SSEE, since the fading estimation errors  $\Delta y_{k,1}$  and  $\Delta y_{k,L-1}$  in the numerators of these two equations, in general, have different values. Equations (10a) and (10b) indicate that the fading estimation error,  $\Delta y_{k,1}$  or  $\Delta y_{k,L-1}$ , in the numerator used to compute the SSEE is always adjacent to the fading effect,  $y_{k,0}$  or  $y_{k+1,0}$ , multiplied by the factor  $(L-1)$ . When the equation with the larger fading effect multiplied by  $(L-1)$  is selected, the SNR for estimation of the adjacent fading effect,  $y_{k,1}$  or  $y_{k,L-1}$ , should normally be larger, leading to a more accurate fading estimate and hence a smaller fading estimation error. Therefore, the equation, Eqn.

(10a) or (10b), with the larger fading effect,  $y_{k,0}$  or  $y_{k+1,0}$ , multiplied by the factor  $(L-1)$  should normally result in a smaller SSEE and hence should be used for fading estimation of  $y_{k,1}$  or  $y_{k,L-1}$ .

The algorithm to implement the proposed technique starts with the fading estimates of  $\hat{y}_{k,0}$  and  $\hat{y}_{k+1,0}$  from Eqns. (6a) and (6b), respectively. The magnitudes  $|\hat{y}_{k,0}|$  and  $|\hat{y}_{k+1,0}|$  are computed and the larger one is selected. Linear interpolation is then used for initial estimation of the fading effect,  $y_{k,1}$  or  $y_{k,L-1}$ , depending on whether  $|\hat{y}_{k,0}|$  or  $|\hat{y}_{k+1,0}|$  is larger. If  $|\hat{y}_{k,0}|$  is larger than  $|\hat{y}_{k+1,0}|$ , the value  $\hat{y}_{k,1}$  is computed using Eqn. (7), otherwise the value  $\hat{y}_{k,L-1}$  is computed instead. In the previous description, the value  $\hat{y}_{k,1}$  (Eqns. 7 to 10a) has been used and so the former assumption is made hereafter. The estimate  $\hat{y}_{k,1}$  is then used to compensate for the fading effect on the received data symbol  $r_{k,1}$  using Eqn. (8). The compensated symbol  $\hat{r}_{k,1}$  is threshold detected to give the detected symbol  $\hat{d}_{k,1}$ , which is a possible vector in the 16QAM signal constellation. The detected symbol  $\hat{d}_{k,1}$  is then used to re-estimate  $y_{k,1}$  as

$$\tilde{y}_{k,1} = r_{k,1} / \hat{d}_{k,1} \quad (11)$$

The process repeats but now with  $\hat{y}_{k,0}$  replaced by  $\tilde{y}_{k,1}$  and for the estimate of  $y_{k,2}$  or  $y_{k,L-1}$ , depending on whether  $|\tilde{y}_{k,1}|$  or  $|\hat{y}_{k+1,0}|$  is larger. Clearly, since  $y_{k,1}$  has a stronger time correlation with both  $y_{k,2}$  and  $y_{k,L-1}$  than  $y_{k,0}$  has, replacing  $\hat{y}_{k,0}$  by  $\tilde{y}_{k,1}$  in the process should normally lead to a more accurate estimate of  $y_{k,2}$  or  $y_{k,L-1}$ , provided that  $\hat{y}_{k,0}$  and  $\tilde{y}_{k,1}$  have been correctly estimated. The whole process repeats until all data symbols within the received signal have been detected.

#### IV. SIMULATION RESULTS AND DISCUSSIONS

A series of Monte Carlo computer simulation tests has been carried out to assess the proposed technique on the BER performances of the PSA-16QAM system shown in Fig. 1 in the light shadowed, the average shadowed and the heavy shadowed Rician fading channels corrupted with AWGN. In the tests, the transfer function of the premodulation and postdemodulation filters in cascade has a raised cosine rolloff of 0.5, and the normalized Doppler spreads of  $f_D T = 2.5 \times 10^{-2}$  and  $f_D T = 5 \times 10^{-2}$  have been used. The SNR is taken as

$$SNR = E_b / N_o = \frac{E_d \times (L-1) + E_p}{M \times (L-1) \times N_o} \quad (12)$$

where  $E_d$  and  $E_p$  are the average transmitted energy per data symbol and pilot symbol, respectively, and  $M$  is the number of information bits carried per data symbol. For 16QAM,  $M = 4$  and  $E_p = 1.8 \times E_d$ , and hence

$$SNR = E_b / N_o = \frac{(L+0.8) \times E_d}{4 \times (L-1) \times N_o} \quad (13)$$

For the purpose of comparison, the results using linear interpolation on the pilot symbols for fading estimation and compensation [1,4] are also present and indexed by a '[P]' in the legend of the figures.

The simulation results of the BER performances of the PSA-16QAM system in the light shadowed Rician fading channels with different frame lengths  $L$  are shown in Fig. 4. In the slower fading environment with  $f_D T = 2.5 \times 10^{-2}$ , Fig. 4(a) shows that using the proposed technique for fading estimation, there is no error floor under all conditions tested. However, when linear interpolation is used, high error floors occur at  $BER = 1.5 \times 10^{-2}$ ,  $7 \times 10^{-2}$  and  $10^{-1}$  with  $L = 20, 35$  and  $50$ , respectively. It can also be seen in Fig. 4(a) that using linear interpolation, the practical BER of  $10^{-3}$  cannot

be achieved with  $L = 20, 35$  and  $50$ . However, the proposed technique can achieve a BER of  $10^{-3}$  with  $L = 20, 35$  and  $50$  at SNR = 26 dB, 28 dB and 30 dB, respectively, requiring 5 - 9 dB power more than that required by using linear interpolation with  $L = 5$ . It should be noticed that with  $L = 50$ , the bandwidth redundancy is only 2%, which is a decade lower than the 20% redundancy with  $L = 5$ . In the faster fading environment with  $f_D T = 5 \times 10^{-2}$ , Fig. 4(b) shows that under the SNRs tested, a BER of  $10^{-3}$  can only be achieved using the proposed technique with  $L = 5$ . With  $L = 20, 35$  and  $50$ , the technique can provide a BER of  $10^{-2}$  at SNR = 19 dB, 21.5 dB and 25 dB, respectively. However, it can be seen in Fig. 4(b) that using linear interpolation with  $L = 20, 35$  and  $50$ , irreducible error floors occur at BERs of around  $10^{-1}$ , rendering the quality of transmission hardly acceptable.

Fig. 4 shows that the proposed technique performs significantly better than linear interpolation with longer frame lengths and faster fading rates. Here the accuracy of the fading estimates on the data symbols obtained using linear interpolation on the pilot symbols are degraded by the weakened time correlation between the fading effects on the data symbols and those on the pilot symbols. The longer is the frame length or the faster is the fading rate, the weaker is the time correlation and so the less accurate are the resultant fading estimates. Since the proposed technique employs the data symbols as well as the pilot symbols for fading estimation, a stronger time correlation between the fading effects on the data symbols and pilot symbols will lead to more accurate fading estimation and better system performances. However, Fig. 4 shows that at low SNRs, the proposed technique is inferior to linear interpolation. This is because the fading estimates obtained using the data symbols (Eqns. 6a and 6b) are less accurate than those obtained using the pilot symbols. And like the other data-aided techniques, the performances of the technique

are degraded by the error propagation of incorrect data detection at low SNRs (Eqn. 11). These result in inferior performances.

In the average shadowed Rician fading channels, the BER performances of the system are shown in Fig. 5. With  $f_D T = 2.5 \times 10^{-2}$ , Fig. 5(a) shows that using the proposed technique, no error floor occurs and a BER of  $10^{-3}$  can be achieved with  $L = 5, 20, 35$  and  $50$ . Although error floors do occur with the faster fading rate of  $f_D T = 5 \times 10^{-2}$  as shown in Fig. 5(b), the proposed technique can substantially lower the error floors, achieving a BER of  $10^{-3}$  with  $L = 5$  and a BER of  $10^{-2}$  with  $L = 20, 35$  and  $50$ .

In the heavy shadowed Rician fading channels, Fig. 6 shows that the BER performances of the system are poor. This is because of the heavy shadowing loss in the fading channels. With  $f_D T = 2.5 \times 10^{-2}$ , Fig. 6(a) shows that the proposed technique can achieve a BER of  $10^{-2}$  with  $L = 20$  and considerably lower the error floors with  $L = 35$  and  $50$ . Shorter frame lengths have been used in the tests with the faster fading rate of  $f_D T = 5 \times 10^{-2}$  and the results are shown in Fig. 6(b). It can be seen that the proposed technique can considerably lower the error floors of the system in all cases.

All these results have shown that the proposed fading estimation technique requires a very low bandwidth redundancy to transmit the pilot symbols, yet providing satisfactory BER performances in the shadowed Rician fading environments. Therefore, the technique is obviously the better choice in the bandwidth-limited PSA systems.

## V. CONCLUSIONS

A novel data-aided fading estimation technique has been proposed for use in the shadowed Rician fading environments. The proposed technique employs both pilot and data symbols to obtain smaller SSEEs for the data symbols. Monte Carlo computer simulation has been used to assess the technique on the BER performances of a PSA-16QAM system. The results have shown that the technique requires a very low bandwidth redundancy to provide satisfactory BER performances, and can substantially lower the error floors of the conventional PSA systems. In the light shadowed Rician fading environment with  $f_d T = 2.5 \times 10^{-2}$ , the technique requires only a 2% bandwidth redundancy to achieve a BER of  $10^{-3}$  at a SNR of 30 dB.

## REFERENCES

- [1] M. L. Moher and J. H. Lodge, "TCMP-A modulation and coding strategy for Rician fading channels," *IEEE J. Select. Areas Commun.*, vol. 7, no. 9, pp. 1347-1355, Dec. 1989.
- [2] A. Aghamohammadi, H. Meyr, and G. Asheid, "A new method for phase synchronization and automatic gain control of linearly modulated signals on frequency-flat fading channels," *IEEE Trans. Commun.*, vol. 39, no. 1, pp. 25-29, Jan. 1991.
- [3] J. K. Cavers, "An analysis of pilot symbol assisted modulation for Rayleigh fading channels," *IEEE Trans. Veh. Technol.*, vol. 40, no. 4, pp. 686-693, Nov. 1991.
- [4] S. Sampei and T. Sunaga, "Rayleigh fading compensation for QAM in land mobile radio communications," *IEEE Trans. Veh. Technol.*, vol. 42, no. 2, pp. 137-147, May 1993.
- [5] C. L. Liu and K. Feher, "Pilot-symbol aided coherent M-ary PSK in frequency-selective fast Rayleigh fading channels," *IEEE Trans. Commun.*, vol. 42, no. 1, pp. 54-62, Jan. 1994.

- [6] K. Y. Tsie and A. H. Aghvami, "High level Trellis-coded modulation with slow frequency hopping for land mobile communications," *IEEE Trans. Veh. Technol.*, vol. 43, no. 1, pp. 147-155, Feb. 1994.
- [7] H. K. Lau and S. W. Cheung, "A pilot symbol-aided technique used for digital signals in multipath environments," *Proc. IEEE Int'l Conf. on Commun.*, pp. 1126-1130, New Orleans, USA, May 1994.
- [8] Y. Kamio and S. Sampei, "Performance of a Trellis-coded 16QAM/TDMA system for land mobile communications," *IEEE Trans. Veh. Technol.*, vol. 43, no. 3, pp. 528-536, Aug. 1994.
- [9] D. Subasinghe-Dias and K. Feher, "A coded 16 QAM scheme for fast fading mobile radio channels," *IEEE Trans. Commun.*, vol. 43, no. 5, pp. 1906-1916, May 1995.
- [10] G. T. Irvine and P. J. McLane, "Symbol-aided plus decision-directed reception for PSK/TCM modulation on shadowed mobile satellite fading channels," *IEEE J. Select. Areas Commun.*, vol. 10, no. 8, pp. 1289-1299, Oct. 1992.
- [11] H. K. Lau and S. W. Cheung, "A fade-compensation technique for digital land mobile satellite systems," *Int'l Journal Of Satellite Communications*, vol. 14, pp. 341-349, 1996.
- [12] C. Loo and N. Secord, "Computer models for fading channels with applications to digital transmission," *IEEE Trans. Veh. Technol.*, vol. 40, pp. 700-707, Nov. 1991.

**TABLE**

Table 1. Shadowed Rician channel model parameters

Parameters	Light Shadowing	Average Shadowing	Heavy Shadowing
$b_0$	0.158	0.126	0.0631
$\mu_0$	0.115	-0.115	-3.91
$\sqrt{d_0}$	0.115	0.161	0.806

## FIGURES

Fig. 1 Block diagram of system

Fig. 2 Frame structure

Fig. 3 Shadowed Rician fading model

Fig. 4 BER performances in light shadowed Rician fading channels with different values of  $L$ .

(a)  $f_D T = 2.5 \times 10^{-2}$

(b)  $f_D T = 5 \times 10^{-2}$

Fig. 5 BER performances in average shadowed Rician fading channels with different values of  $L$ .

(a)  $f_D T = 2.5 \times 10^{-2}$

(b)  $f_D T = 5 \times 10^{-2}$

Fig. 6 BER performances in heavy shadowed Rician fading channels with different values of  $L$ .

(a)  $f_D T = 2.5 \times 10^{-2}$

(b)  $f_D T = 5 \times 10^{-2}$

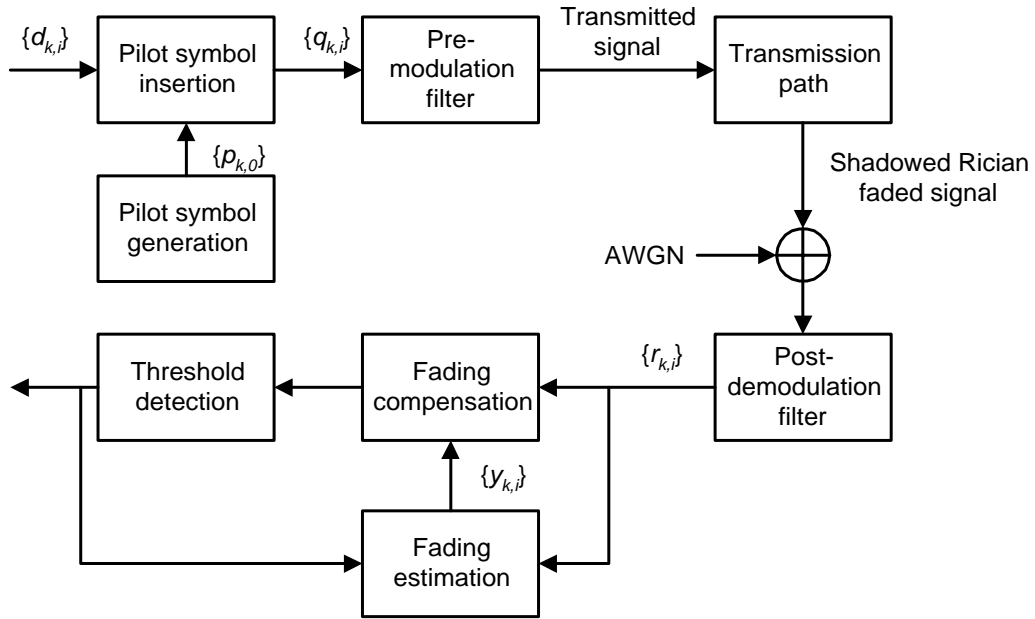


Fig. 1 Block diagram of system

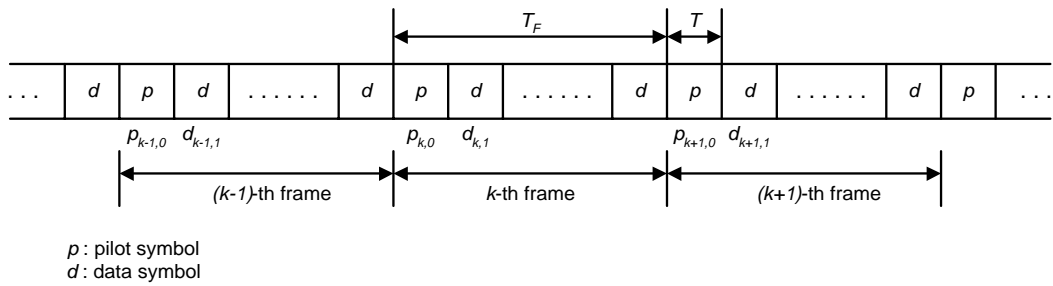


Fig. 2 Frame structure

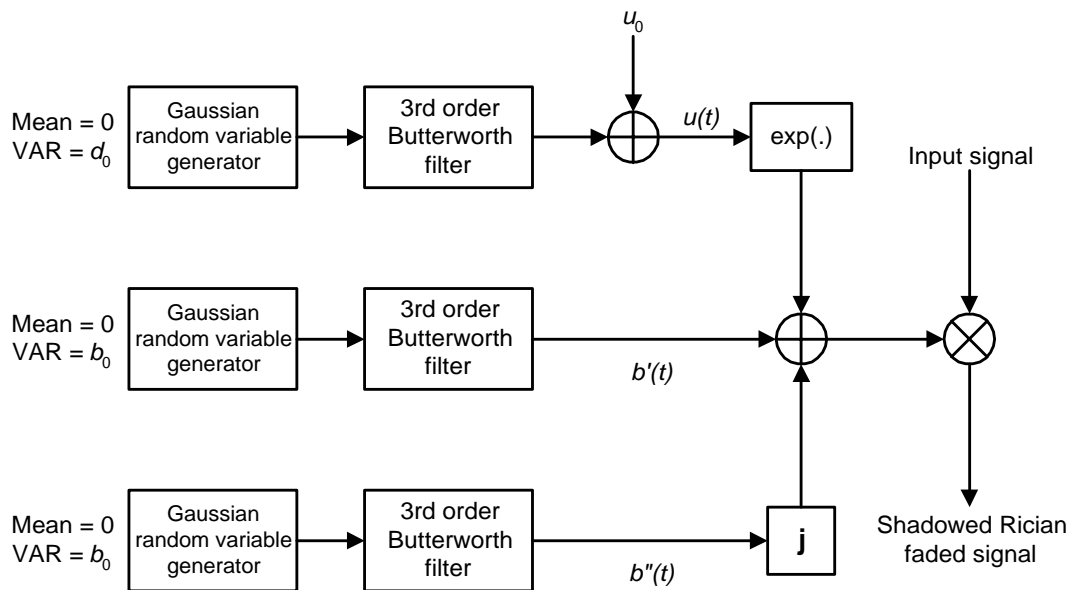
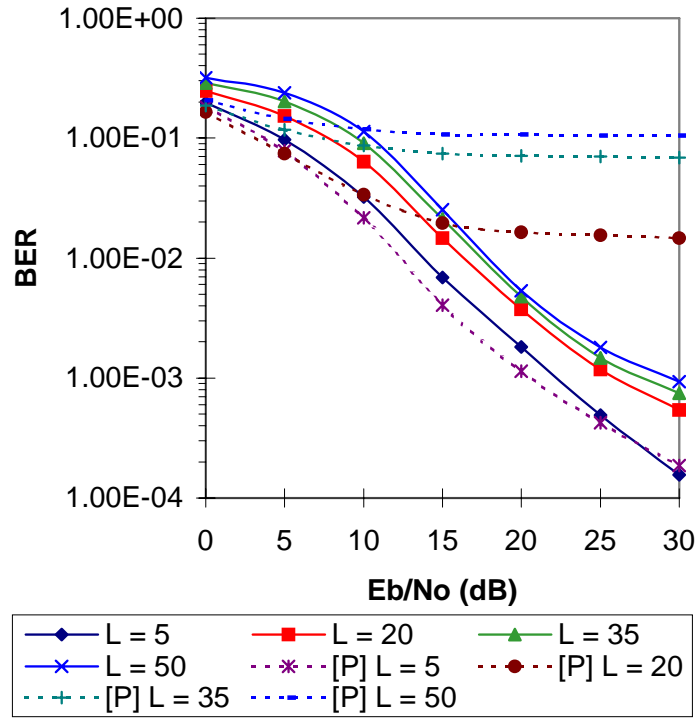
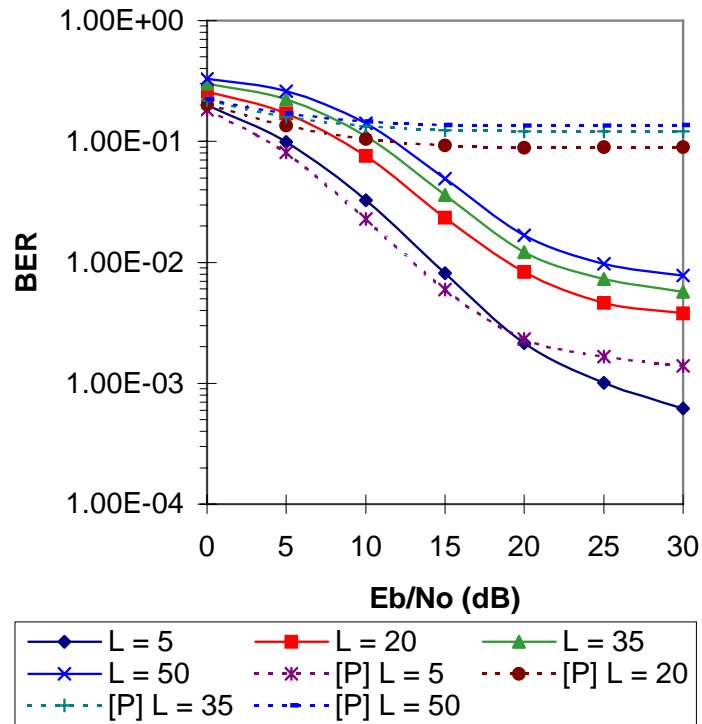


Fig. 3 Shadowed Rician fading model

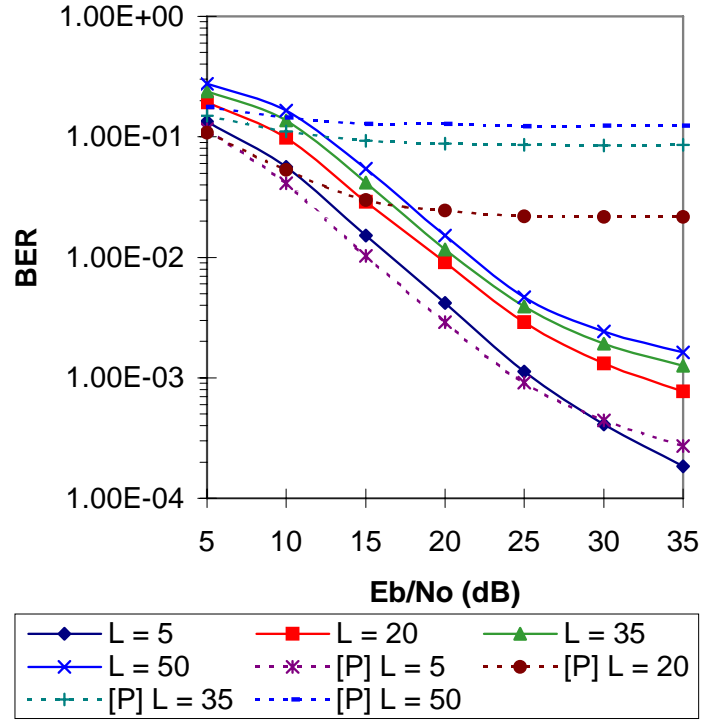


(a)  $f_d T = 2.5 \times 10^{-2}$

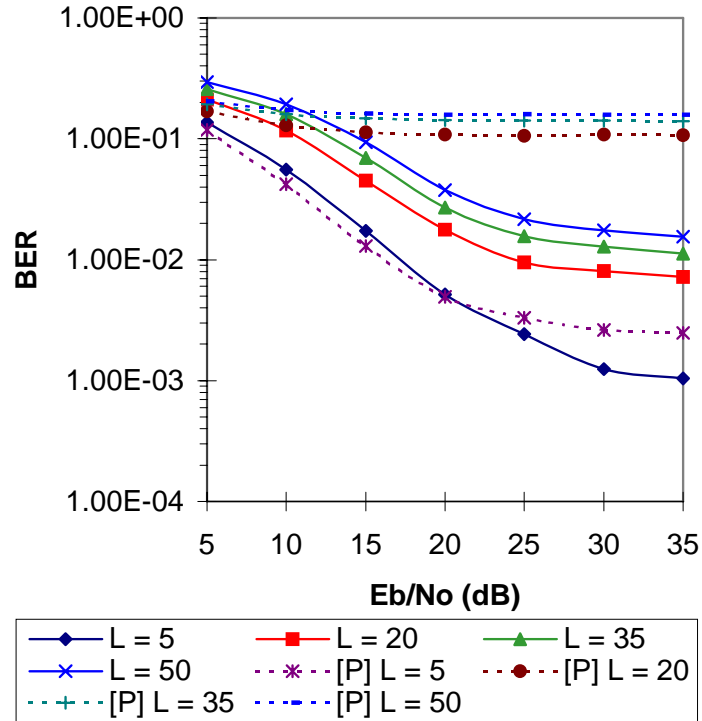


(b)  $f_d T = 5 \times 10^{-2}$

Fig. 4 BER performances in light shadowed Rician fading channels with different values of  $L$ .

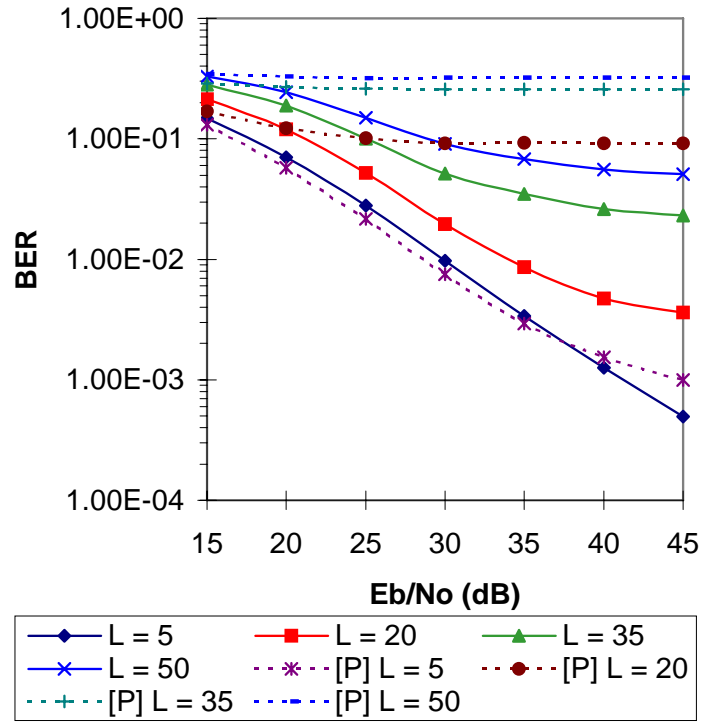


(a)  $f_d T = 2.5 \times 10^{-2}$

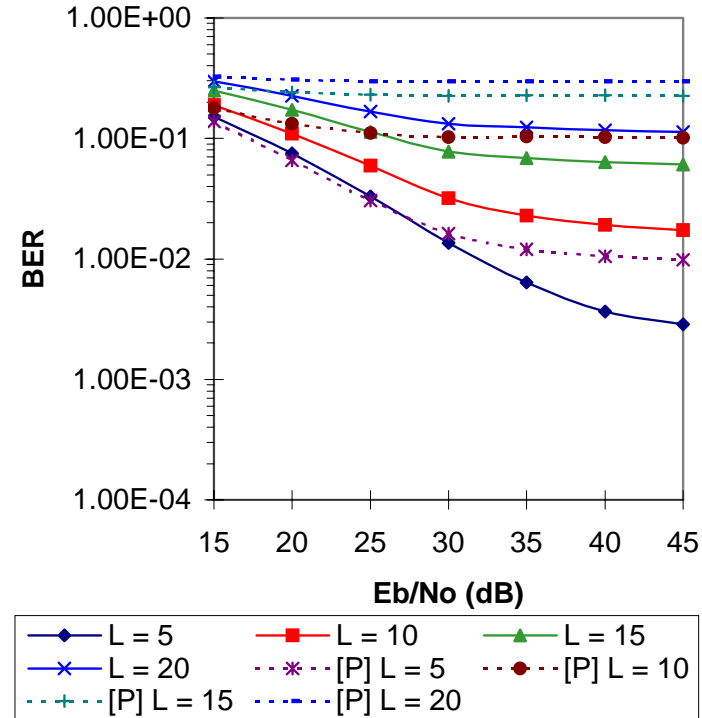


(b)  $f_d T = 5 \times 10^{-2}$

Fig. 5 BER performances in average shadowed Rician fading channels with different values of  $L$ .



(a)  $f_d T = 2.5 \times 10^{-2}$



(b)  $f_d T = 5 \times 10^{-2}$

Fig. 6 BER performances in heavy shadowed Rician fading channels with different values of  $L$ .

## AUTHORS' BIOGRAPHIES



**Man-Hung Ng** received a BSc degree in Computer Studies from City University of Hong Kong in 1991. He worked as a computer programmer in Hong Kong from 1991 to 1995. In 1996, he obtained a MSc degree in Communication and Radio Engineering from King's College London. He joined the University of Hong Kong as a research assistant in 1997, and completed a PhD degree in mobile communications in 2001. He is going to join Lucent Technologies in the UK as a standard engineer.



**Sing-Wai Cheung** was born in Hong Kong. He received the BSc degree in Electrical and Electronic Engineering from Middlesex University, U.K. in 1982 and the PhD degree from Loughborough University of Technology, U.K. in 1986. From 1986-1988, he was a post-doctorate research assistant in the Communications Research Group of King's College, London University. During 1988-1990, he was with the Radio and Satellite Communications Division in British Telecom Research Laboratories (now Adastral Park). He joined the Department of Electrical and Electronic Engineering at the University of Hong Kong in 1990 and is now an Associate Professor. He contributes regularly courses on mobile and satellite communications systems. His current research interests include modulation, coding, fading compensation and diversity for mobile and satellite communications systems.